5. P. HING and P. W. McMILLAN, *J. Mater. Sci.* 8 (1973) 1041.
6. L. J. BROUTMAN and R. H. KROCK, "Modern Composite Materials" (Addison-Wesley, Reading, MA, USA, 1976) p. 13.
7. R. T. DEHOFF and F. N. RHINES, "Quantitative Microscopy" (McGraw-Hill, New York, 1968).
8. J. D. PROVANCE and J. S. HUEBNER, *J. Amer. Ceram. Soc.* 54 (1971) 147.
9. J. M. STEVELS, "Handbuch der Physik", Vol. XX, edited by S. W. Flugge (Springer-Verlag, Berlin, 1957) p. 350.
10. E. H. KERNER, *Proc. Phys. Soc. London* B69 (1956) 802.
11. B. ABELES, SHENG PING, M. D. COUTTS and Y. ARIE, *Adv. Phys.* 24 (1975) 407.

Received 28 February
and accepted 10 May 1979

D. CHAKRAVORTY
B. N. KESHAVARAM
A. VENKATESWARAN
Materials Science Programme,
Indian Institute of Technology,
Kanpur, India

The lowest laser–Raman active accordion (ALR) type oscillations in crystalline polymers

The longitudinal accordion-type mode (LAM) frequencies of crystals of linear polymers with the chains perpendicular to the lamella surface are imagined as corresponding to the longitudinal eigenfrequencies of an ideally elastic rod of length D having the maximum amplitude at its ends. In such a case the eigenmodes have a wavelength $\lambda = 2D, 2D/2, 2D/3 \ldots$. Among them only those corresponding to $\lambda_1, \lambda_3 \ldots$ having a node in the centre of the rod are Raman active. They can be labelled ALR1, ALR2,... since only these wavelengths λ_{Rn}, frequencies $\nu_{Rn} = c_{ac}/\lambda_{Rn}$ or wave numbers ν^*_{Rn}/c_{opt} are observed in the laser-Raman scattering experiment. Here $c_{ac} = (E/\rho)^{1/2}$ is the sound velocity and $c_{opt} = 3 \times 10^8$ m sec^{-1} is the light velocity. The ratio of the corresponding eigenfrequencies or wave numbers is expected to be 1:3:5:.... Small deviations can be easily attributed to end groups, chain folds, strong repulsive forces, and similar small effects which shift the eigenfrequencies of the elastic rod to a lower value if they contribute a mass, and to a higher value if they contribute an additional restoring force.

The experiments agree to a large extent with this view if one is concerned with linear polymers having a zig-zag conformation in the crystal lattice and, hence, a very high axial elastic modulus. Strobl and Eckel [1] report on linear polyethylene (PE) wave number values $\nu^*_{R1} = 24.2 \pm 0.3$ cm^{-1} and $\nu^*_{R2} = 69.0 \pm 1$ cm^{-1}. Their ratio is 2.85 which is so close to 3 that one does not worry too much about the model. The situation deteriorates a little if one considers the true maxima of polarizability derivatives which according to Krimm and Hsu [2] shifts the ALR1 wave number to 24.9 ± 0.3 cm^{-1} thus yielding for the ratio of the second to the first accordion-type Raman frequencies the value, 2.77 which is a little further away from 3 than 2.85.

The situation is much less satisfactory with polymers which crystallize with the chains in helical conformation, as for instance polypropylene (PP) [3], polyoxymethylene (POM) [4], and poly(ethylene oxide) (POE) [5]. The ALR1 wave numbers differ so much from those calculated for independent elastic rods with the known density ρ_c and elastic modulus E_c that one has to consider the addition of restoring forces at the ends of the crystalline rods [6] or the coupling of rods through the amorphous layers [6, 7]. It turned out that the model of coupled rods reproduces the data in a simpler manner and in better agreement with the physics of the system [7].

The first and second ALR scattering wave numbers were measured on PEO. Shepherd and coworkers [8–10] report $\nu^*_{R1} = 9.2 \pm 0.3$ cm and $\nu^*_{R2} = 19.0 \pm 1$ cm^{-1} with the ratio 2.06 which differs so much from 3 that it is certain that something must be wrong with the model. The situation becomes still more extreme if one calculates the true maxima of polarizability derivative which, according to Krimm and Hsu [2], shifts the wave number ν^*_{R1} by 10% and that of ν^*_{R2} by 3% to higher values. With the so-corrected values, $\nu^*_{R1} = 10.12 \pm 0.3$ cm^{-1} and $\nu^*_{R2} = 19.57 \pm 1$ cm^{-1}, one has the ratio $\nu^*_{R2}/\nu^*_{R1} = 1.93 \pm 0.15$ which is even lower than 2.

 0022–2461/79/122994–05$02.50/0

It turns out, however, that these data can be easily interpreted by the model of coupled rods with purely elastic response of the crystalline rod and the amorphous layer between consecutive rods [7]. The period of the structure is L, the long period as derived from small-angle X-ray scattering. The volume crystallinity of the system is $\alpha_v = D/L$. The Raman active eigenmodes have a node in the centre of the rod and one in the centre of the amorphous layer. The nth harmonic ALRn has $2(n-1)$ additional modes if one labels the basic mode with two nodes as the harmonic mode with $n = 1$. The boundary condition for the ALR type of oscillation reads

$$\begin{aligned}
\tan y &= -u \tan zy \\
y &= 2\pi(D/2)/\lambda = (\pi/2)(D/D') \\
u &= (\rho_c E_c/\rho_a E_a)^{1/2} \\
z &= (lD)(\rho_a E_c/\rho_c E_a)^{1/2} \\
&= (1/\alpha_v - 1)(\rho_a/\rho_c)u \\
l &= L - D \\
D' &= \lambda/2.
\end{aligned}$$

Note that the inactive oscillations are obtained if, in the boundary conditions (Equation 1), one changes the sign in front of u and/or replaces u by $1/u$. In such a way one obtains, for each number of nodes per period L, two LAM oscillations. Only one among the four eigenmodes corresponding to $2n-1$ and $2n$ nodes is a Raman active mode labelled as ALRn because only in the $2n$th oscillation does one find one node in the centre of the rod and one in the centre of the amorphous layer as is necessary for Raman activity.

This becomes evident by considering a very rough approximation which, although not numerically exact, shows the trend expected. In the hypothetical case of equal density of the crystalline and amorphous layers, $\rho_c = \rho_a$, one can easily study the influence of the elastic modulus ratio, E_c/E_a, on the laser–Raman active oscillations of the coupled rod system as shown in Fig. 1. If this ratio is 1, the whole section containing the crystal core of thickness D and on each side an amorphous layer of thickness $l/2$ oscillates as a uniform unit. One has the wavelengths $2L$, $2L/2$, $2L/3$, . . . as shown in Fig. 1b. The first two Raman active modes have the wavelength $2L/2$

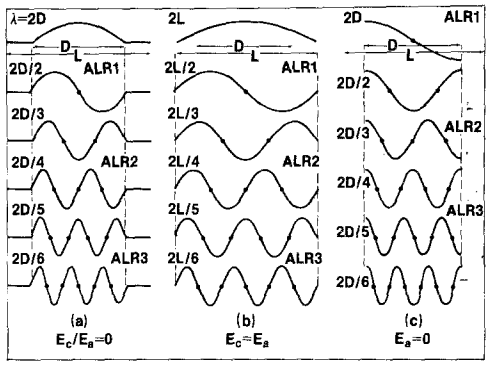

Figure 1 The longitudinal accordion modes (LAM) with a node in the centre of the amorphous layers, and the Raman active oscillation modes (ALR) of the coupled rod model for $E_c/E_a = 0$ (a), $E_c = E_a$ (b) and of the independent rod model (c). In all cases it was assumed that $\rho_c = \rho_a$, $\alpha_v = D/L < 1$. The Raman active oscillations have a node in the centre of the rod.

(ARL1) and $2L/4$ (ARL2) with the ratio of the corresponding frequencies ν_{R2}/ν_{R1} or wave numbers ν^*_{R2}/ν^*_{R1} equal to 2 and not to 3 as expected for freely oscillating independent rods.

The same ratio is obtained in the case when the elastic modulus of the amorphous component is so high that the ratio E_c/E_a goes to zero. In such a limiting case the amorphous component does not oscillate at all so that the boundary between the crystalline rod and the amorphous layer is a node of the oscillation. This yields the longitudinal accordion-type eigenmodes with the wavelengths $2D$, $2D/2$, $2D/3$, $2D/4$ . . . (Fig. 1a). Since D is smaller than L the wavelengths are shorter and the corresponding frequencies higher than in the case of equal E_c and E_a. The first two Raman active oscillations have a wavelength $2D/2$ (ALR1) and $2D/4$ (ALR2). Their ratio is again 2 and not 3. But note that the eigenfrequencies are very much different in both cases, proportional to $1/L$ in the former (Fig. 1b) and in $1/D$ in the latter case (Fig. 1a).

In the other extreme of the very soft amorphous layer with E_c/E_a going to infinity, the coupled rod model does not yield any oscillation of the crystalline rods because practically all the oscillation energy is concentrated in the amorphous layers. With increasing E_c/E_a ratio, the oscillation amplitude of the rods goes to zero. In such a case the coupled rod model cannot be applied. The rods practically do not oscillate and all the nodes, besides the central node of the crystal, are in the

amorphous layers. The situation is the complete reverse of the case $E_c/E_a = 0$ shown in Fig. 1a. The eigenfrequencies of such a system have practically nothing to do with the thickness of the crystalline areas. They depend only on the goemetry of the amorphous layers in exactly the same manner as the eigenfrequencies at $E_c/E_a = 0$ depend on the geometry of the crystalline layers.

In the limit $E_a/E_c = 0$, the crystalline sections are completely independent of each other. They actually oscillate as individual rods without any coupling among them. Hence one obtains from the actual wavelengths of the LAM the values $2D$, $2D/2$, $2D/3$ . . . (Fig. 1c). The first two Raman active nodes correspond to a wavelength $2D$ (ALR1) and $2D/3$ (ALR2). The wave numbers of the LAM eigenfrequencies of the isolated rod are identical to those of the coupled rod with E_a infinitely large. But their elongation pattern and hence their Raman activity is completely different so that the wavelengths of ALR1 and ALR2 of both cases do not agree. In the case of coupled rods with $E_a = \infty$ each even LAM oscillation is Raman active while in the case of independent rods only the odd LAM oscillations are Raman active. The same difference shows up in the ratio of the wave numbers which is 1:3:5 . . . in the case of independent rods, and 1:2:3 . . . in the case of a very large elastic modulus of the amorphous component which couples the oscillations of the rods.

One sees that the main effect of the coupling of oscillating rods is the shift in the Raman activity. While with independent rods the Raman active LAM oscillations have the odd indices $1, 3, 5, \ldots$, the coupling makes the LAM oscillations with even indices $2, 4, 6, \ldots$ Raman active. As a consequence, the ratio of the frequencies or wave numbers of the first two ALR frequencies is 2 and not 3 as in the case of freely oscillating elastic rods. With higher E_c/E_a ratio this value must go from 2 to 3 because in the limit of every high E_c/E_a ratio the actual oscillation approaches that of independent rods. This transition cannot be performed on the coupled rod model with purely elastic amorphous and crystalline medium. One has to introduce the more complicated viscoelastic mechanical response of the amorphous layer in order to be able to extend the coupled rod model sufficiently close to the limit of isolated rods. The viscosity of the amorphous medium must be so high that except that at the centre of the amorphous layer no other nodes can develop, and at the same time the elasticity must be so low that no substantial coupling is to be considered. The results of such a model will be published soon.

From this extremely rough estimate one concludes that the observed ν^*_{R3}/ν^*_{R1} values will be between 2 and 3 depending on the ratio E_c/E_a. This is in good general agreement with experimental data which in the case of PE and PEO show a value below 3. In Fig. 2 are plotted the results ν^*_{R2}/ν^*_{R1} and ν^*_{R3}/ν^*_{R1} versus E_c/E_a calculated for $\rho_c = 1.23$ and $\rho_a = 1.12\,\mathrm{g\,cm^{-3}}$ corresponding to PEO. The parameter is the volume crystallinity $\alpha_v = D/L$. All curves pass through the value 2 and 3, respectively, at $E_c/E_a = \rho_a/\rho_c = 0.9106$ which makes equal the dynamic rigidity E_ρ of the crystalline and amorphous component. At such a point the whole section with the length L oscillates as a uniform material with one node in the centre and one at the boundary of the section without any dependence on the crystallinity. The higher nodes are equally spaced through the whole medium, i.e. at a distance $L/2n$.

Before one starts to compare the theoretical predictions with the experimentally observed values one has to consider the limitations of the coupled rod model. The first one concerns the location of the nodes which besides that in the

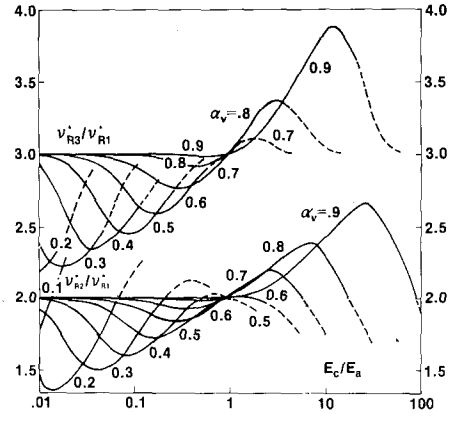

Figure 2 The ratios ν^*_{R2}/ν^*_{R1} and ν^*_{R3}/ν^*_{R1} as function of E_c/E_a for $\rho_c = 1.23$ and $\rho_a = 1.12\,\mathrm{g\,cm^{-3}}$, corresponding to PEO with the volume crystallinity $\alpha_v = D/L$ as the parameter. Broken lines represent the cases where at least one node on each side of the central node is in the amorphous instead of in the crystalline layer.

centre of the amorphous layer, are supposed to be all located inside the crystalline core of the sample. There is no problem with the basic ALR1 oscillation which has only one node in the crystal and one located in the centre of the amorphous segment. But with very low crystallinity some of the nodes of ALR harmonics which are supposed to be inside the crystal may be situated outside the crystalline core. This happens as soon as the wavelength of the second ALR oscillation is larger than D. With the third ALR oscillation the condition is $\lambda_{R3} > D/2$, with the nth ALR harmonics $\lambda_{Rn} > D/(n-1)$. Since such cases have to be excluded the results obtained in such regions are marked in Fig. 2 by a broken line. One sees that with the lower α_v the excluded area extends from $E_c/E_a = \infty$ down to a lower value of this ratio. At the smallest $\alpha_v = 0.1$ practically all the range of this ratio is excluded, i.e. for all the values E_c/E_a considered, the new nodes are situated outside the very small crystal and hence do not represent a possible oscillation mode of the system. A good picture about this effect can be derived from the graphs in Fig. 1. In the case of $E_c/E_a = 0$ all the nodes are always inside the crystal. In the case $E_c/E_a = 1$, the crystallinity $\alpha_v = 2/3$ just keeps the nodes up to ALR3 inside or at the outer boundary of the crystalline rod. Any higher eigenmode has at least one node at each side of the rod outside the crystal and hence has to be excluded. This happens earlier with lower α_v.

The other concern relates to the intrinsic limitation of the coupled rod model at high values of the ratio E_c/E_a. As already mentioned, the rods in the limit $E_a \to 0$ are completely independent without any coupling and hence do not oscillate at all. In approaching this limit the major part of the energy of oscillation is concentrated in the amorphous layers while the crystals oscillate with such a low amplitude that they are practically at rest. Hence the coupled rod model fails at high E_c/E_a ratio and does not yield at this limit the independent rod results with the ratio $\nu^*_{R2}/\nu^*_{R1} = 3$ and $\nu^*_{R3}/\nu^*_{R1} = 5$. The failure occurs earlier with lower crystallinity α_v, i.e. with a larger difference between D and L. In the plots of ν^*_{R2}/ν^*_{R1} and ν^*_{R3}/ν^*_{R1} in Fig. 2 this situation starts to show up in the falling off of the curves corresponding to fixed crystallinity. The fall off prevents the curves approaching the above-mentioned limits of 3 and 5. One sees that the effect is most conspicuous at small α_v. At large α_v the upward trend extends over a larger range of E_c/E_a values so that one can guess how the limits 3 and 5 will be approached. The maximum of the ν^*_{R3}/ν^*_{R1} and ν^*_{R3}/ν^*_{R1} curves moves to higher E_c/E_a values with higher crystallinity. This effect can be understood if one considers that the development of a large amplitude of the oscillation in the amorphous layer is made easier by a large width $l/L = (L-D)/L = 1-\alpha_v$ of the layer. If the layer is very thin, α_v close to 1, a higher E_c/E_a ratio must be approached in order to achieve the same oscillating energy.

This type applies no limitation to the small values $E_c/E_a < 1$ because in such a case the major part of the oscillation is in the crystal core and only a minor part in the more rigid amorphous layers. Hence, one can accept without reservation the ν^*_{R2}/ν^*_{R1} and ν^*_{R3}/ν^*_{R1} curves in the region from $E_c/E_a = 0$ almost up to the falling off of the curves at $E_c/E_a > 1$.

With the above corrections in mind one sees that the ratio ν^*_{R2}/ν^*_{R1} starts with the value 2 at very small ratio E_c/E_a, becomes slightly smaller than 2 when one approaches $E_c\rho_c/E_a\rho_a = 1$ and goes to the limit 3 at $E_c/E_a = \infty$. Similarly the ratio ν^*_{R3}/ν^*_{R1} starts with the value 3 and after $E_c\rho_c/E_a\rho_a = 1$, approaches the limit 5 of freely oscillating rods. The influence of the crystallinity is minor in the whole range of interest of E_c/E_a between slightly below 1 up to infinity. Since it has been shown previously that the ν^*_{R1} values of PEO are in good agreement with the known value of $E_c = 10$ GPa if one takes $\alpha_v = 0.7$ and E_a between 20 and 30 GPa, one expects that the same parameters will also yield the observed ratio $\nu^*_{R2}/\nu^*_{R1} = 1.93 \pm 0.15$. It turns out that such a value is indeed obtained at E_c/E_a between 1/2 and 1/3.5 which yields E_a between 20 and 35 GPa in very good agreement with the former analysis of ALR1 of PEO.

The situation with PE is a little different because the volume crystallinity 0.8 and the E_c/E_a ratio about 25 locate the system in the area where the coupled rod model with purely elastic components fails to represent the physical situation sufficiently well. The ν^*_{R2}/ν^*_{R1} curve falls off at $E_c/E_a = 6$. Hence the ascending section of the curve does not extend far enough to include the PE sample. However, one sees that the envelope of

the ascending sections of the curves corresponding to α_v above 0.6 steadily approaches the supposed limit 3 corresponding to freely oscillating rods. Hence, from a rather general point of view the location of $\nu^*_{R2}/\nu^*_{R1} = 2.83$ or 2.77 between 2 and 3 is in perfect agreement with the results of the coupled rod model as represented in Fig. 2. Moreover, the proper density ratio $\rho_a/\rho_c = 0.853$ shifts all the lines in Fig. 2 to the left which makes the agreement still better. The smaller value, 2.77 at $E_c/E_a = 25$ or even at $E_c/E_a = 17$ is indeed located on the common envelope steadily rising to the limit 3 of the free rods corresponding to $E_a = 0$.

References

1. G. R. STROBL and R. ECKEL, *Prog. Colloid Polymer Sci.* **62** (1977) 9.
2. S. KRIMM and S. L. HSU, *J. Polymer Sci. Polymer Phys. Ed.* **16** (1978) 2105.
3. S. L. HSU, S. KRIMM, S. KRAUSE and G. S. Y. YEH, *J. Polymer Sci.* **B14** (1976) 195.
4. J. F. RABOLT and B. FANCONI, *J. Polymer Sci.* **B15** (1977) 121.
5. A. HARTLEY, Y. K. LEUNG, C. BOOTH and I. W. SHEPHERD, *Polymer* **17** (1976) 354.
6. S. L. HSU, G. W. FORD and S. KRIMM, *J. Polymer Sci. Polymer Phys. Ed.* **15** (1977) 1769.
7. A. PETERLIN, *J. Appl. Phys.* **50** (1979) 838.
8. A. HARTLEY, U. K. LEUNG, C. BOOTH and I. W. SHEPHERD, *Polymer* **17** (1976) 354.
9. A. J. HARTLEY, Y.-K. LEUNG, J. McMAHON, C. BOOTH and I. W. SHEPHERD, *ibid.* **18** (1977) 1190.
10. J. M. EDWARD, R. D. MULLEY, G. A. PAPE, C. BOOTH and I. W. SHEPHERD, *ibid* **18** (1977) 1190.

Received 22 March
and accepted 10 May 1979

A. PETERLIN
Polymer Science and Standards Division,
National Bureau of Standards,
Washington,
D.C. 20234
USA

The role of nickel in the one-coat vitreous enamelling system

In the industrial enamelling of ferrous metals it has always been necessary to add other metals, nickel and cobalt, to the system to obtain a satisfactory enamel–metal bond, i.e., one which failed in a cohesive manner. In the two-coat system these metals are added as oxides, "adhesion oxides", to the glass frit and in one-coat enamelling a thin layer of nickel is applied to the steel prior to the application of the enamel slip. There is evidence that this nickel deposit should be discontinuous to achieve a satisfactory bond between the enamel and the metal [1]. The precise function of this nickel flash has not been satisfactorily explained, but more recent publications suggest that it acts in at least two ways. When present the flash increases the proportion of Fe_3O_4 in the oxide scale which forms on the steel surface prior to the fusion of the enamel [2, 3]. Also the crystallographic structure of the nickel–iron alloy which forms during the later stages of firing is believed to promote good adherence [2,4]. These explanations which require particular chemical or physical conditions at the interface are not satisfactory in view of the demonstration by Klomp that bonds which fail cohesively could be formed between ceramics and metals without the aid of an intermediate layer at the interface [5]. The work reported here suggests that the nickel flash promotes bonding because it prevents the accumulation of hydrogen at the enamel–metal interface rather than its influence on the oxidation of the steel or the crystallographic properties of the alloy formed with the iron.

In a systematic investigation of the one-coat enamelling system various alterations were made in the pretreatment of the metal, including omitting the nickel flash. The differences observed are clearly shown in Fig. 1. Where the nickel flash was present the normal enamelling reaction sequence occurred; during the initial stages of firing the surface of the steel is oxidized by the atmosphere, the enamel then fuses, dissolves the oxide scale and further oxidation of the steel then occurs. This latter stage is accompanied by a marked roughening of the enamel–metal interface and the iron oxide formed in this second stage also diffuses into the enamel layer. In the absence of a nickel flash only the first stage oxidation had taken place and a separation of the two layers had occurred, resulting in a 30 μm gap. This gap must have formed when the enamel dissolved the

0022–2461/79/122998–03$02.30/0